# Complex Chaotic Dynamics of the Double-Bell Attractor

M.S. PAPADOPOULOU, I.M. KYPRIANIDIS, and I.N. STOUBOULOS
Physics Department
Aristotle University of Thessaloniki
Thessaloniki, 54124
GREECE
mpapa@physics.auth.gr, kyprianidis@physics.auth.gr, stouboulos@physics.auth.gr

*Abstract:* - In this paper a novel non-autonomous 4th order chaotic oscillator was investigated. This oscillator consists of a nonlinear resistance $R_N$ and a negative conductance $G_n$. We have studied the dynamics of the circuit for various values of the input sinusoidal signal $v_s(t)$ in the low frequency area, both theoretically and experimentally. We have demonstrated the birth and catastrophe of the Double-Bell strange attractor for different frequencies values, as the amplitude $V_o$ of the input signal varies. This work is a precursor of future investigation of circuit's application in secure communication systems.

*Key-Words:* - Driven circuit, Double-Bell attractor, Chaos, Spectrum analysis, Secure communication.

## 1 Introduction

Chaos can be defined as a system that diverges exponentially from initial positions varying by a small degree [1]. It has been found to be useful in analyzing many problems such as information processing, high-performance circuits and devices etc.

There are two types of chaotic systems, autonomous and non-autonomous [2]. Although there are many known autonomous chaotic oscillators [3-11] very few non-autonomous have been introduced in the literature [12-18]. Non-autonomous chaotic circuits form a class of systems which produce chaos while being driven by an external time varying source. The amplitude and frequency of the sinusoidal signal both contribute to the chaotic dynamics of the system.

In this paper the low frequency response of a 4th order non autonomous, nonlinear circuit has been studied. The electronic circuit consists of two active elements, one linear negative conductance and one nonlinear resistor of N-type symmetrical v-i characteristic. The circuit also contains two capacitances $C_1$ and $C_2$, two inductances $L_1$ and $L_2$, and a sinusoidal voltage $v_s(t)$.

## 2 Proposed Driven Chaotic Oscillator

The circuit we have studied is shown in Fig.1. In Figs. 2(a) and 2(b) we can see the nonlinear resistance implementation and its v-i characteristic, while in Figs.2(c) and 2(d) the negative conductance implementation and its v-i characteristic are presented, respectively.

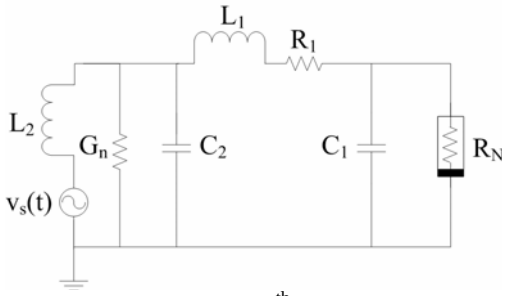


Fig.1. The implemented 4th order driven electric circuit.

The state equations of the system are:

$$\frac{dv_{C1}}{dt}=\frac{1}{C_1}\left(i_{L1}-i\right) \quad (1)$$

$$\frac{dv_{C2}}{dt}=-\frac{1}{C_2}\left(G_n\cdot v_{C2}+i_{L1}-i_{L2}\right) \quad (2)$$

$$\frac{di_{L1}}{dt}=\frac{1}{L_1}\left(v_{C2}-v_{C1}+R_1 i_{L1}\right) \quad (3)$$

$$\frac{di_{L2}}{dt}=\frac{1}{L_2}\left(v_{C2}+R_2 i_{L2}-v_s(t)\right) \quad (4)$$

where the nonlinear function i is described by

$$i=g(v_{C1})=G_b v_{C1}+0.5(G_a-G_b)(|v_{C1}+B_p|-|v_{C1}-B_p|) \quad (5)$$

$v_s(t)$ is the input sinusoidal signal, while $R_2$ denotes the internal resistance of the source.

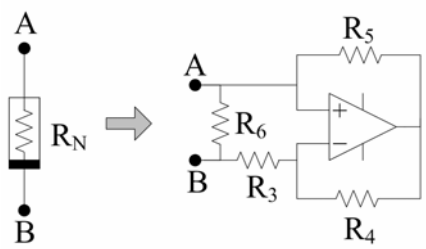


(a) Circuit's Elements: $R_3$=1.0KΩ, $R_4$=15.5KΩ, $R_5$=4.1KΩ, $R_6$=297Ω.

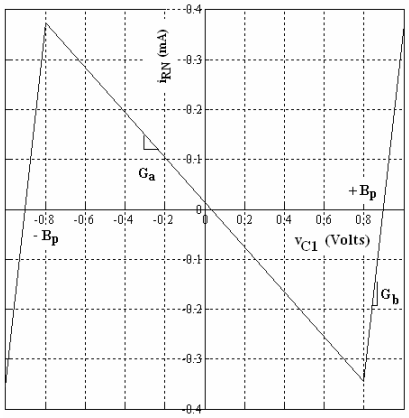


(b)

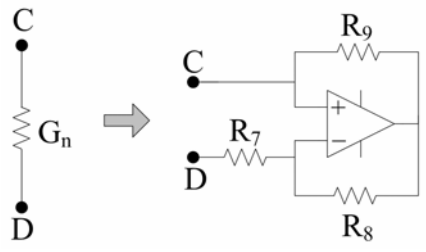


(c) Circuit's Elements: $R_7$=$R_8$=$R_9$=2.0KΩ

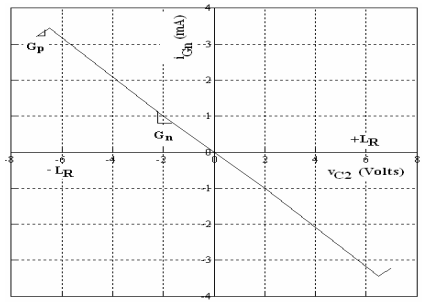


(d)

Fig.2. (a) Nonlinear resistance implementation (b) v-i characteristic of N-type nonlinear element $R_N$ (c) Negative conductance implementation and (d) v-i characteristic of negative conductance $G_n$.

The parameters of the circuit are considered unchangeable during our study. More particularly, we have that: $L_1$ = 100mH, $L_2$ = 100mH, $C_1$ = 33nF, $C_2$ = 75nF, $R_1$ =1KΩ, $G_n$ = -0.50mS = -$G_p$, $L_R$ =7.5V, $G_a$ = -0.35mS, $G_b$ = 5.0mS and $B_p$ = 0.8V.

# 3 Low Frequency Response

We have studied system's response in low frequencies range. Particularly, the theoretical-simulation and experimental phase portraits $v_{C2}$ vs. $v_{C1}$ for f=30Hz and f=35Hz and various values of the amplitude $V_o$ of input sinusoidal signal $v_s(t)$ are shown in subsections 3.1 and 3.2, respectively. Moreover, we present the spectrum analysis, both theoretically and experimentally, for f=30Hz (subsection 3.1) and f=35Hz (subsection 3.2).

All the experimental phase portraits were taken with HM507 Hameg Analog/ Digital oscilloscope, while spectrums were taken with TDS2024 TEKTRONIX Digital oscilloscope.

## 3.1 The Double-Bell Attractor for f = 30Hz

In Figs.3, 5, 7 and 9 we can see the theoretical and experimental phase portraits $v_{C2}$ vs. $v_{C1}$ for f =30Hz and various values of the amplitude $V_o$ of the input sinusoidal signal $v_s(t)$. Primarily, we can see the birth of the Double-Bell attractor (Fig.3) for $V_o$=0.60V.

Hereupon, the evolution of Double-Bell attractor is presented (Figs. 5 and 7), as the two separate Bells penetrate to each other (Fig.7).

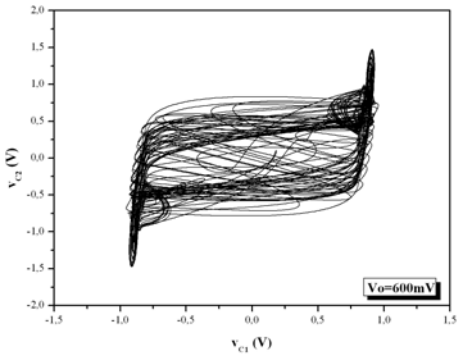


(a) Simulation

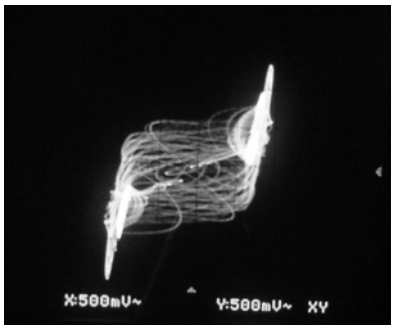


(b) Experimental

Fig.3. Phase portrait $v_{C2}$ vs. $v_{C1}$ for $V_o$=0.60V.

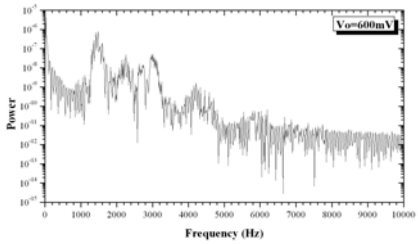


(a) Simulation

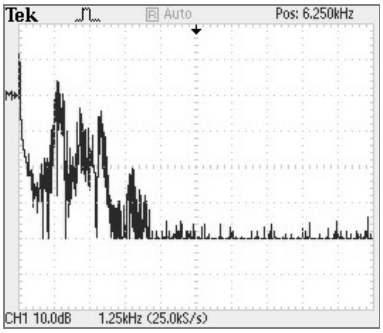


(b) Experimental

Fig.4. Spectrum of $v_{c2}(t)$ for f=30Hz and $V_o$=0.60V.

Finally, the catastrophe of the above phenomenon is occured (Fig.9) for high amplitudes of the input signal.

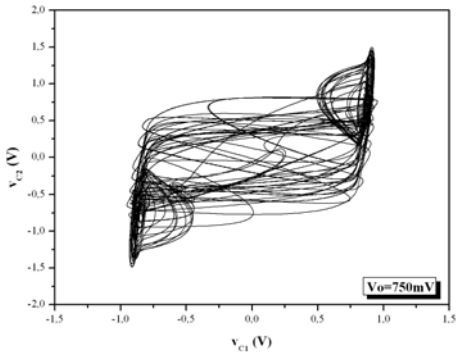


(a) Simulation

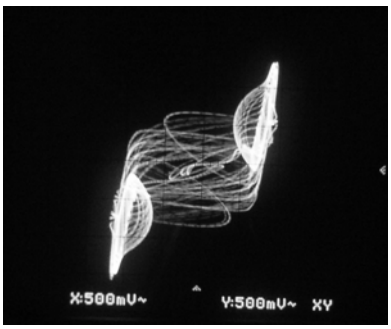


(b) Experimental

Fig.5. Phase portrait $v_{C2}$ vs. $v_{C1}$ for $V_o$=0.75V.

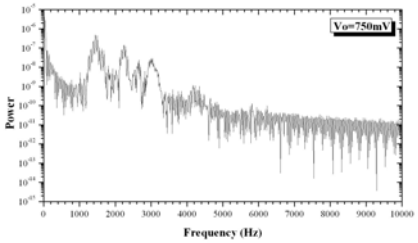


(a) Simulation

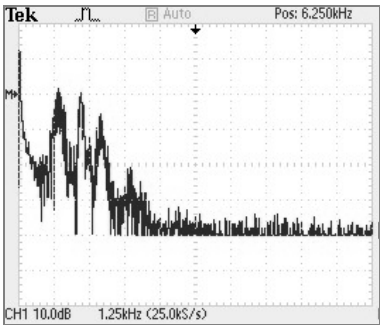


(b) Experimental

Fig.6. Spectrum of $v_{c2}(t)$ for f=30Hz and $V_o$=0.75V.

In Figs.4, 6, 8 and 10 we observe the theoretical and experimental spectrums of $v_{c2}(t)$ for f =30Hz and various values of the input amplitude $V_o$.

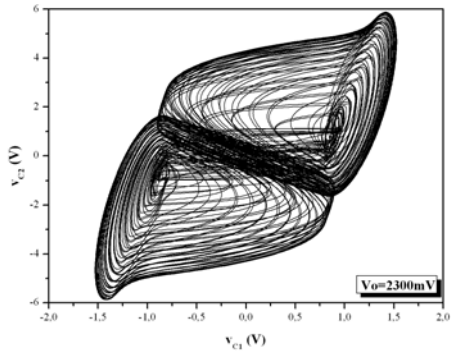


(a) Simulation

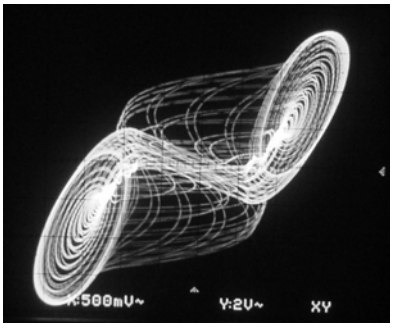


(b) Experimental

Fig.7. Phase portrait $v_{C2}$ vs. $v_{C1}$ for $V_o$=2.30V.

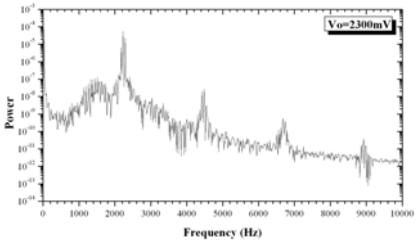


(a) Simulation

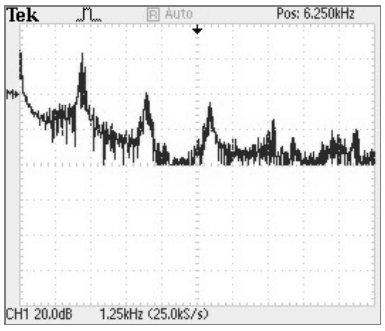


(b) Experimental

Fig.8. Spectrum of $v_{c2}(t)$ for f=30Hz and $V_o$=2.30V.

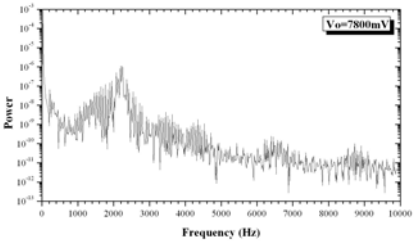


(a) Simulation

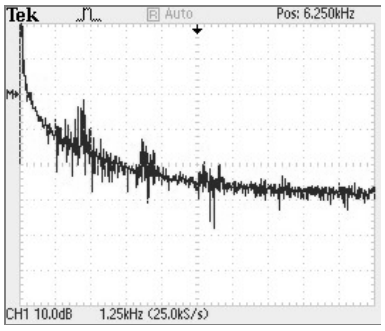


(b) Experimental

Fig.10. Spectrum of $v_{c2}(t)$ for f=30Hz and $V_o$=7.80V.

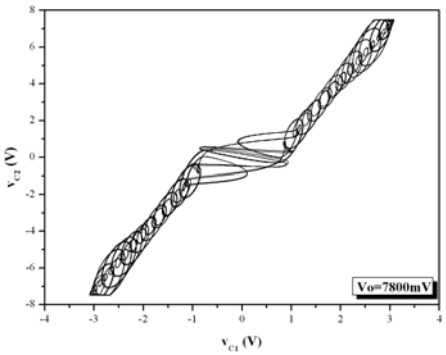


(a) Simulation

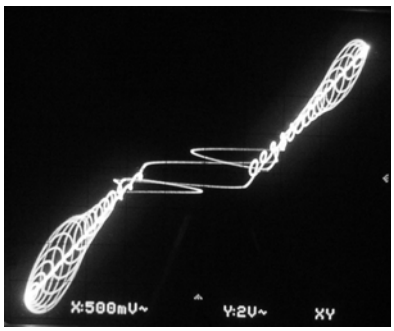


(b) Experimental

Fig.9. Phase portrait $v_{C2}$ vs. $v_{C1}$ for $V_o$=7.80V.

## 3.2 The Double-Bell Attractor for f = 35Hz

In this subsection (Figs.11-18) the same procedure for f=35Hz, as in for f=30Hz (§3.1), is repeated.

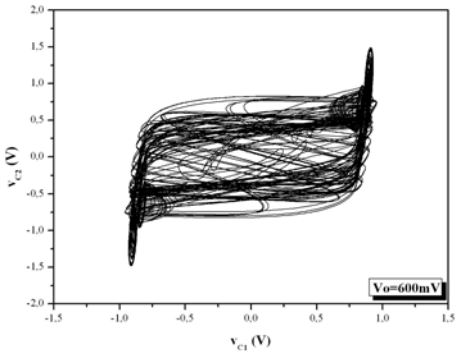


(a) Simulation

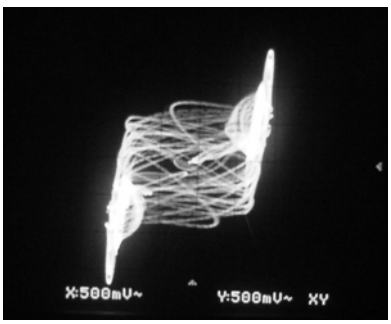


(b) Experimental

Fig.11. Phase portrait $v_{C2}$ vs. $v_{C1}$ for $V_o$=0.60V.

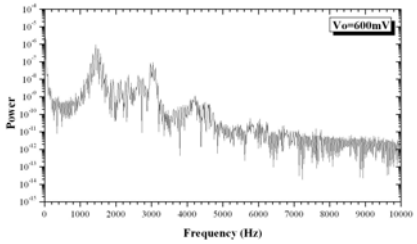


(a) Simulation

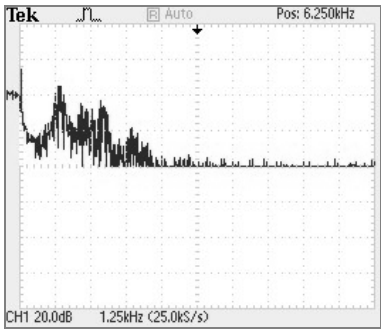


(b) Experimental

Fig.12. Spectrum of $v_{c2}(t)$ for f=35Hz and $V_o$=0.60V.

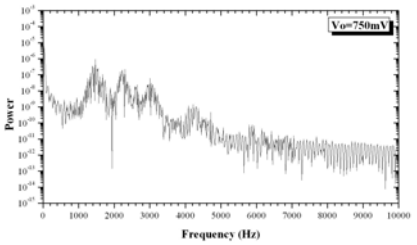


(a) Simulation

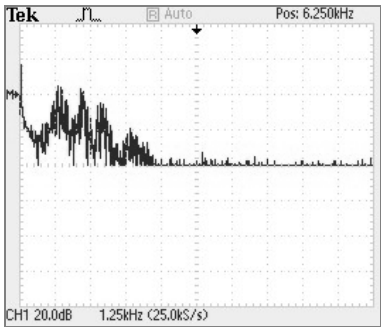


(b) Experimental

Fig.14. Spectrum of $v_{c2}(t)$ for f=35Hz and $V_o$=0.75V.

So, the phase portraits for amplitude $V_o$ equal to 0.60V, 0.75V, 2.30V and 7.50V are presented in Figs.11, 13, 15 and 17, respectively. The spectrums of $v_{c2}(t)$ for the same values of amplitude $V_o$ of the input signal are also given in Figs.12, 14, 16 and 18.

In those figures we can observe simultaneously the theoretical and experimental spectrums of $v_{c2}(t)$ for the driven 4th order proposed circuit.

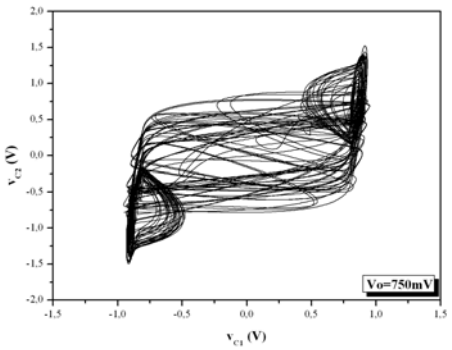


(a) Simulation

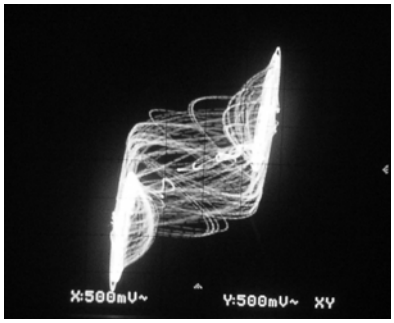


(b) Experimental

Fig.13. Phase portrait $v_{C2}$ vs. $v_{C1}$ for $V_o$=0.75V.

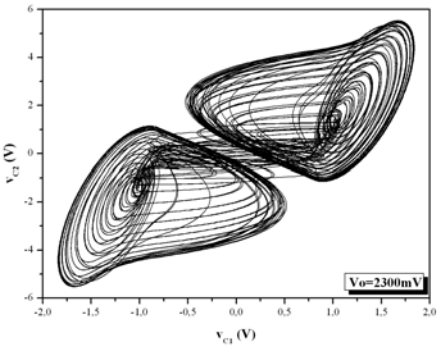


(a) Simulation

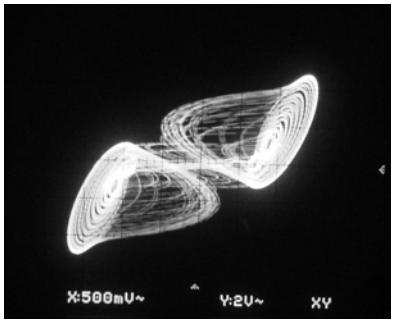


(b) Experimental

Fig.15. Phase portrait $v_{C2}$ vs. $v_{C1}$ for $V_o$=2.30V.

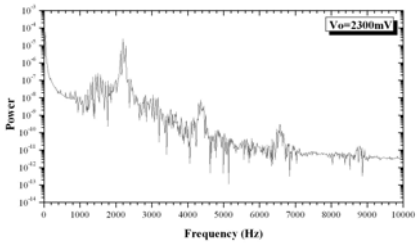


(a) Simulation

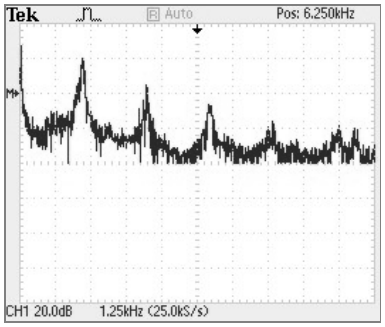


(b) Experimental

Fig.16. Spectrum of $v_{c2}(t)$ for f=35Hz and $V_o$=2.30V.

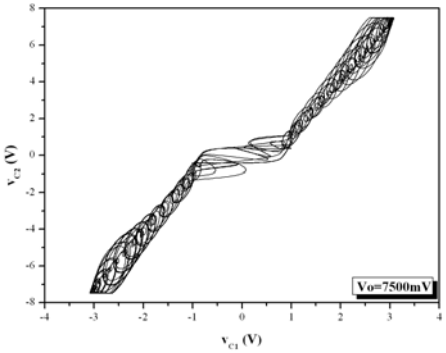


(a) Simulation

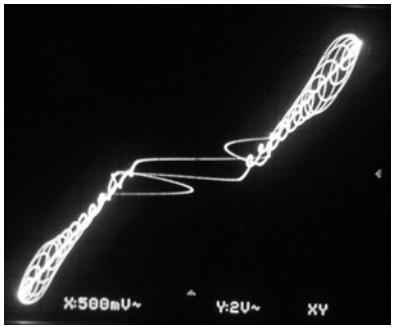


(b) Experimental

Fig.17. Phase portrait $v_{C2}$ vs. $v_{C1}$ for $V_o$=7.50V.

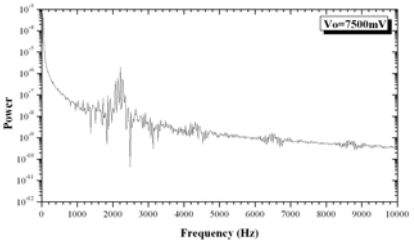


(a) Simulation

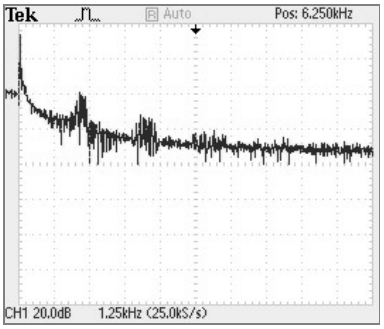


(b) Experimental

Fig.18. Spectrum of $v_{c2}(t)$ for f=35Hz and $V_o$=7.50V.

We can clearly see that the evolution of Double-Bell attractor for f=35Hz is exactly the same, as in for f=30Hz.

# 4 Chaotic and Periodic Attractors

Thereafter, we perform numerical simulations of the above system using Runge-Kutta algorithm. In subsections 4.1 and 4.2 we present the Poincare sections $(v_{C2})_p$ vs. $(i_{L2})_p$ for f =30Hz and f =35Hz, respectively. The data interval is equal to 0.05.

## 4.1 Poincare Sections for f = 30Hz

In Figs.19-22 we observe the Poincare sections $(v_{C2})_p$ vs. $(i_{L2})_p$ for f =30Hz.

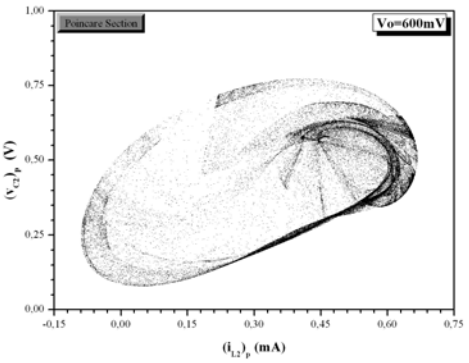


Fig.19. Poincare section $(v_{C2})_p$ vs. $(i_{L2})_p$ for $V_o$=0.60V.

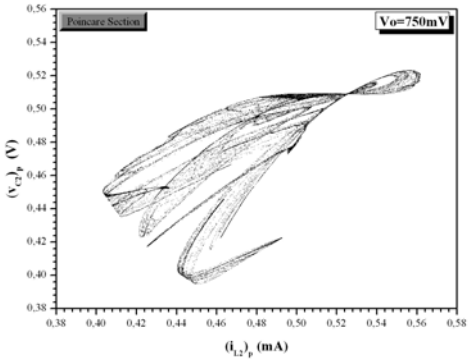


Fig.20. Poincare section $(v_{C2})_p$ vs. $(i_{L2})_p$ for $V_o$=0.75V.

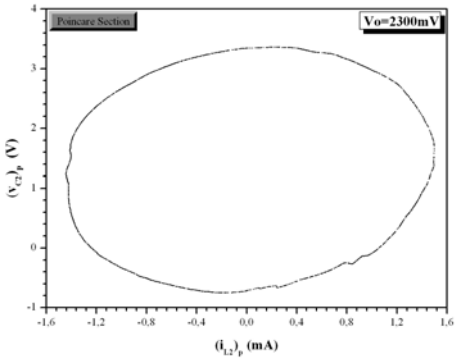


Fig.21. Poincare section $(v_{C2})_p$ vs. $(i_{L2})_p$ for $V_o$=2.30V.

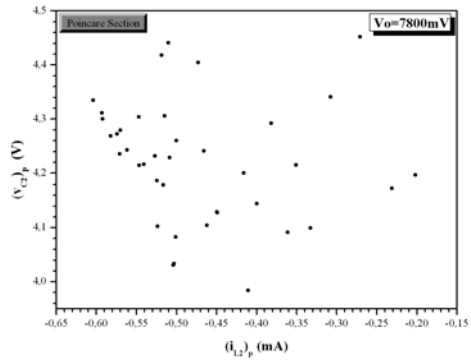


Fig.22. Poincare section $(v_{C2})_p$ vs. $(i_{L2})_p$ for $V_o$=7.80V.

The values of the amplitude of the input sinusoidal signal and the parameters of numerical simulations are the same as in subsection 3.1.

We can see from Figs.19 ($V_o$=0.60V) and 20 ($V_o$=0.75V) that the attractors seem to be chaotic, while for $V_o$=2.30V (Fig.21) and $V_o$=7.80V (Fig.22) the attractors are quasiperiodic and periodic (with period p-39), respectively.

## 4.2 Poincare Sections for f = 35Hz

In Figs.23-26 we present the Poincare sections $(v_{C2})_p$ vs. $(i_{L2})_p$ for f =35Hz and various values of the amplitude $V_o$ of $v_s(t)$. The values of $V_o$ and the parameters of numerical simulations are the same as in subsection 3.2.

Similarly, as in for f=30Hz (subsection 4.1), we have a strong indication that the attractors for $V_o$=0.60V (Fig.23) and $V_o$=0.75V (Fig.24) could be chaotic, while for $V_o$=2.30V (Fig.25) and $V_o$=7.50V (Fig.26) are quasiperiodic and periodic (with period p-31), respectively.

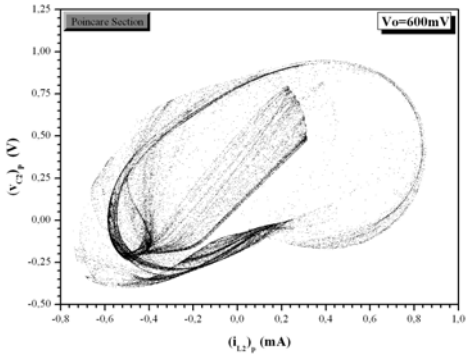


Fig.23. Poincare section $(v_{C2})_p$ vs. $(i_{L2})_p$ for $V_o$=0.60V.

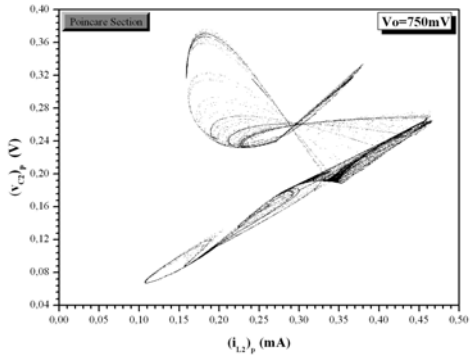


Fig.24. Poincare section $(v_{C2})_p$ vs. $(i_{L2})_p$ for $V_o$=0.75V.

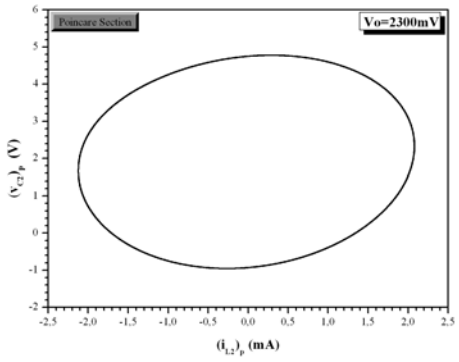


Fig.25. Poincare section $(v_{C2})_p$ vs. $(i_{L2})_p$ for $V_o$=2.30V.

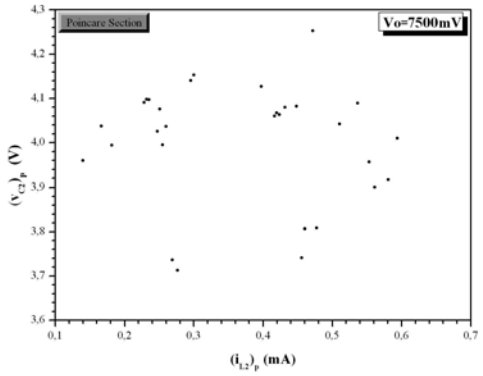


Fig.26. Poincare section $(v_{C2})_p$ vs. $(i_{L2})_p$ for $V_o$=7.50V.

# 5 Conclusion

A sinusoidal-driven chaotic oscillator with a non linear resistor of N-type v-i characteristic and a negative conductance was proposed. We have studied the dynamics of the circuit for various values of the input sinusoidal signal $v_s(t)$ in the low frequency area, both theoretically and experimentally.

In particularly, for f=30Hz, we have observed the birth of the Double-Bell strange attractor for $V_o$=0.60V (Fig.3), its evolution for $V_o$=0.75V (Fig.5) and $V_o$=2.30V (Fig.7), as the two separate Bells merge to each other and finally, the catastrophe of the above phenomenon (Fig.9) for high amplitude values of the input signal. We have also computed and presented the Poincare sections (Figs.19-22) and spectrums of $v_{c2}(t)$ (Figs.4, 6, 8 and 10), from which we are concluding about circuit's dynamic behavior.

Afterwards, we have repeated the same procedure for f=35Hz. Hence, we have seen the birth of the Double-Bell strange attractor (Fig.11), its evolution (Figs.13 and 15) and finally, its catastrophe (Fig.17) for high amplitudes $V_o$ of the input sinusoidal signal. We have also presented the Poincare sections (Figs.23-26) and spectrums of $v_{c2}(t)$ (Figs.12, 14, 16 and 18) of the circuit.

The study of the above system has shown that the theoretical and experimental results agree to each other. We have seen chaotic, quasiperiodic and periodic attractors for various values of the amplitude of the input signal in low frequency area. Those features comprise an optimistic scenario for future investigation of circuit's application in secure communication systems.

*Acknowledgments:*
The authors would like to express their appreciation to the reviewers for their valuable comments and suggestions.

*References:*

[1] Hunt, E., and Johnson, G., Keeping chaos at bay, *IEEE Spectrum*,Vol.30, Issue11, 1993, pp.32-36.

[2] Murali, K., Lakshmanan, M., and Chua, L.O., The simplest dissipative nonautonomous chaotic circuit, *IEEE Transactions on Circuits and Systems-I*, Vol.41, Issue 6, 1994, pp. 462-463.

[3] Elwakil, A.S., and Kennedy, M.P., Construction of classes of circuit-independent chaotic oscillators using passive-only nonlinear devices, *IEEE Transactions on Circuits and Systems-I*, Vol.48, Issue 3, 2001, pp. 289-307.

[4] Kennedy, M.P., Chaos in the colpitts oscillator, *IEEE Transactions on Circuits and Systems-I*, Vol.41, Issue 11, 1994, pp. 771-774.

[5] Namajunas, A., and Tamasevicius, A., Modified Wien-bridge oscillator for chaos, *Electronics Letters*, Vol.31, Issues 5, 1995, pp. 335-336.

[6] Elwakil, A.S., and Kennedy, M.P., Towards a methodology for designing autonomous chaotic oscillators, *Proceedings of the 6th International Specialist Workshop on Nonlinear Dynamics of Electronic Systems NDES'98*, 1998, pp. 79-82.

[7] Stouboulos, I.N., Kyprianidis, I.M., and Papadopoulou, M.S., Experimental study of antimonotonicity in a 4th order nonlinear autonomous electric circuit, *WSEAS Transactions on Circuits and Systems*, Vol.5, Issue 11, 2006, pp. 1662-1668.

[8] Stouboulos, I.N., Kyprianidis, I.M., and Papadopoulou, M.S., Chaotic dynamics and coexisting attractors in a modified Chua's circuit, *WSEAS Transactions on Circuits and Systems*, Vol.5, Issue 11, 2006, pp. 1640-1646.

[9] Kyprianidis, I.M., Stouboulos, I.N., Haralabidis, P. and Bountis T., Antimonotonicity and chaotic dynamics in a fourth-order autonomous nonlinear electric circuit, *International Journal of Bifurcation and Chaos*, Vol.10, No.8, 2000, pp. 1903-1915.

[10] Koliopanos, Ch.L., Kyprianidis, I.M., Stouboulos, I.N., Anagnostopoulos, A.N., and Magafas, L., Chaotic behaviour of a fourth-order autonomous electric circuit, *Chaos Solitons and Fractals*, Vol.16, 2003, pp. 173-182.

[11] Matsumoto, T., Chua, L.O., and Tokunaga, R., Chaos via. Torus Breakdown, *IEEE Transactions Circuits Systems*, Vol.34, 1987, pp. 240-253.

[12] Tanaka, S., Matsumoto, T., and Noguchi, J., Multi-folding: alternative appearance of period-one attractors and chaotic attractors in a driven R-L-diode circuit, *Physics Letters A,* Vol.157, No.1, 1991, pp. 37-43.

[13] Tanaka, S., Noguchi, J., Higuchi, S., and Matsumoto, T., A repeated appearance of period-l attractor in a driven R-L-diode circuit: experimental and theoretical bifurcation analysis, *IEICE Transactions on Fundamentals of Electronics, Communications and Computer Sciences,* Vol.E74-A, No.6, 1991, pp. 1406-1413.

[14] Kennedy, M.P., Chua, L.O., Van der Pol and Chaos, *IEEE Transactions on Circuits and Systems,* Vol.33, Issue 10, 1986, pp. 974-980.

[15] Linsay, P.S., Period doubling and chaotic behavior in a driven anharmonic oscillator, *Physical Review Letters,* Vol.47, No.19, 1981, pp. 1349-1352.

[16] Chua, L.O., Yao, Y., Yang, Q., Devil's staircase route to chaos in a nonlinear circuit, *International Journal of Circuit Theory and Applications,* Vol.14, No.4, 1986, pp. 315-329.

[17] Jeffries, C., and Perez, J., Direct observation of crises of the chaotic attractor in a nonlinear oscillator, *Physical Review A,* Vol.27, No.1, 1983, pp. 601-603.

[18] Ikezi, H., deGrassie, J.S., and Jensen, T.H., Observation of multiple-valued attractors and crises in a driven nonlinear circuit, *Physical Review A,* Vol.28, No.2, 1983, pp. 1207-1209.